JOURNAL OF GEOPHYSICAL RESEARCH, VOL. 112, D23304, doi:10.1029/2007JD008710, 2007

Evidence for a recurring eastern North America upper tropospheric ozone maximum during summer

O. R. Cooper,[1,2] M. Trainer,[3] A. M. Thompson,[4] S. J. Oltmans,[3] D. W. Tarasick,[5] J. C. Witte,[6] A. Stohl,[7] S. Eckhardt,[7] J. Lelieveld,[8] M. J. Newchurch,[9] B. J. Johnson,[3] R. W. Portmann,[3] L. Kalnajs,[10] M. K. Dubey,[11] T. Leblanc,[12] I. S. McDermid,[12] G. Forbes,[13] D. Wolfe[3] T. Carey-Smith,[14,15] G. A. Morris,[16] B. Lefer,[17] B. Rappenglück,[17] E. Joseph,[18] F. Schmidlin,[19] J. Meagher,[3] F. C. Fehsenfeld,[3] T. J. Keating,[20] R. A. Van Curen,[21] and K. Minschwaner[22]

Received 27 March 2007; revised 29 June 2007; accepted 30 August 2007; published 11 December 2007.

[1] Daily ozonesondes were launched from 14 North American sites during August 2006, providing the best set of free tropospheric ozone measurements ever gathered across the continent in a single season. The data reveal a distinct upper tropospheric ozone maximum above eastern North America and centered over the southeastern USA. Recurring each year, the location and strength of the ozone maximum is influenced by the summertime upper tropospheric anticyclone that traps convectively lofted ozone, ozone precursors and lightning NO_x above the southeastern USA. The North American summer monsoon that flows northward along the Rocky Mountains is embedded within the western side of the anticyclone and also marks the westernmost extent of the ozone maximum. Removing the influence from stratospheric intrusions, median ozone mixing ratios (78 ppbv) in the upper troposphere (>6 km) above Alabama, near the center of the anticyclone, were nearly twice the level above the U.S. west coast. Simulations by an atmospheric chemistry general circulation model indicate lightning NO_x emissions led to the production of 25–30 ppbv of ozone at 250 hPa above the southern United States during the study period. On the regional scale the ozone enhancement above the southeastern United States produced a positive all-sky adjusted radiative forcing up to 0.50 W m^{-2}.

Citation: Cooper, O. R., et al. (2007), Evidence for a recurring eastern North America upper tropospheric ozone maximum during summer, *J. Geophys. Res.*, *112*, D23304, doi:10.1029/2007JD008710.

1. Introduction

[2] Tropospheric ozone is a central trace gas that influences the oxidizing capacity of the troposphere, and is also a strong greenhouse gas, especially in the upper troposphere where ozone changes have a greater impact on surface temperatures [*Forster and Shine*, 1997; *Intergovernmental Panel on Climate Change*, 2001, 2007]. Much of the

[1]Cooperative Institute for Research in Environmental Sciences, University of Colorado, Boulder, Colorado, USA.
[2]Also at Earth System Research Laboratory, NOAA, Boulder, Colorado, USA.
[3]Earth System Research Laboratory, NOAA, Boulder, Colorado, USA.
[4]Department of Meteorology, Pennsylvania State University, University Park, Pennsylvania, USA.
[5]Experimental Studies Research Division, Meteorological Service of Canada, Environment Canada, Downsview, Ontario, Canada.
[6]Science Systems and Applications, Inc., NASA Goddard Space Flight Center, Greenbelt, Maryland, USA.
[7]Norwegian Institute for Air Research, Kjeller, Norway.
[8]Max Plank Institute for Chemistry, Mainz, Germany.
[9]Atmospheric Science Department, University of Alabama in Huntsville, Huntsville, Alabama, USA.
[10]Laboratory of Atmospheric and Space Physics, University of Colorado, Boulder, Colorado, USA.
[11]Los Alamos National Laboratory, Los Alamos, New Mexico, USA.
[12]Table Mountain Facility, Jet Propulsion Laboratory, California Institute of Technology, Wrightwood, California, USA.
[13]Meteorological Service of Canada, Sable Island, Nova Scotia, Canada.
[14]Environment Canada, Downsview, Ontario, Canada.
[15]Now at National Institute of Water and Atmospheric Research Ltd., Wellington, New Zealand.
[16]Department of Physics and Astronomy, Valparaiso University, Valparaiso, Indiana, USA.
[17]Geosciences Department, University of Houston, Houston, Texas, USA.
[18]Department of Physics and Astronomy, Howard University, Washington, D. C., USA.
[19]Wallops Flight Facility, NASA Goddard Space Flight Center, Wallops Island, Virginia, USA.
[20]Office of Air and Radiation, United States Environmental Protection Agency, Washington, D. C., USA.
[21]Atmospheric Processes Research Section, Research Division, California Air Resources Board, Sacramento, California, USA.
[22]Department of Physics, New Mexico Institute of Mining and Technology, Socorro, New Mexico, USA.

0148-0227/07/2007JD008710$09.00

tropospheric ozone burden is produced from anthropogenic emissions [*Levy et al.*, 1997; *Hauglustaine et al.*, 1998], resulting in widespread ozone increases since the late 1800s [*Marenco et al.*, 1994; *Staehelin et al.*, 1994; *Lamarque et al.*, 2005; *Oltmans et al.*, 2006]. The increase of ozone since preindustrial times has produced a global average radiative forcing of 0.35 W m^{-2}. The positive radiative forcing of tropospheric ozone is comparable to that of halocarbons, and twice that of N_2O, but lower than the radiative forcing from CO_2 and CH_4 [*Intergovernmental Panel on Climate Change*, 2001, 2007]. The Intergovernmental Panel on Climate Change assigns a level of understanding of "medium" to tropospheric ozone's radiative forcing, because of its shorter lifetime compared to other greenhouse gases and its large spatial and seasonal variability. The lack of a global-scale free tropospheric ozone monitoring network has prevented researchers from collecting in situ data that can reveal the full spatial and temporal variability of tropospheric ozone on a global or even continental scale.

[3] A recent development in our understanding of tropospheric ozone is the discovery of a summertime ozone maximum within the upper tropospheric anticyclone above the southern United States. The existence of this feature was first suggested by *Li et al.* [2005]. Output from their chemical transport model indicated that the ozone enhancement would be the result of convective lofting of surface ozone, and in situ production by anthropogenic NO_x, lightning NO_x, and in part by HO_x radicals produced from convectively lifted formaldehyde that originates from biogenic isoprene. The ozone could be produced over many days because of the trapping of the ozone precursors in the semipermanent upper tropospheric anticyclone located above eastern North America during summer. Verification of the study was limited by the availability of just five ozonesondes from Huntsville, Alabama. While these sondes did indicate enhanced upper tropospheric ozone, the existence of a horizontally extensive but isolated upper tropospheric ozone maximum could not be confirmed because of the lack of an ozone measurement network across North America.

[4] During summer 2004 the INTEX Ozonesonde Network Study (IONS) experiment provided ozonesondes from multiple sites across eastern North America plus one upwind site at Trinidad Head, California [*Thompson et al.*, 2007b]. *Cooper et al.* [2006] combined the IONS ozonesondes with ozone profiles from MOZAIC commercial aircraft at several US and Canadian airports, and ozone profiles from a lidar in southern California, to produce a more comprehensive set of free-tropospheric ozone profiles across North America. Once the model-calculated stratospheric ozone contribution had been removed from all tropospheric profiles the data did reveal an upper tropospheric ozone enhancement above southeastern Texas, in agreement with *Li et al.* [2005]. On average the upper troposphere of eastern North America contained an additional 16 ppbv of ozone compared to the west coast, with a maximum enhancement of 24 ppbv above Houston, Texas. A detailed study of NO_x sources indicated that lightning produced 78–95% of the NO_x in the upper troposphere above eastern North America, and that 69–84% of the ozone enhancement was due to in situ ozone production from lightning NO_x (ozone production rates of 3–4 ppbv/d) with the remainder due to transport of ozone from the surface or in situ ozone production from other sources of NO_x. Recent work by *Hudman et al.* [2007] reaches similar conclusions regarding the upper tropospheric NO_x budget.

[5] To learn more about the North American free tropospheric ozone distribution, an additional phase of the IONS experiment was conducted during August 2006, which measured for the first time the free tropospheric ozone distribution across North America in a single season, and also provided the best free tropospheric ozone data set ever collected across the continent. This ozonesonde network was specifically designed to quantify (1) the background ozone that flows into western and southern North America, (2) the ozone exported from North America in polluted air masses, and (3) the enhanced ozone mixing ratios in the upper tropospheric anticyclone above the southern USA.

[6] The purpose of the present study is to use the unprecedented spatial and temporal coverage of the August 2006 IONS data to (1) support the recent studies that indicate the presence of an upper tropospheric ozone enhancement above eastern North America during summer and (2) further our understanding of the feature's spatial extent, interannual variability, and its relationship to the North American Monsoon. The analysis begins with an examination of tropospheric ozone across North America using high-quality ozonesonde measurements and a particle dispersion model to remove any recent influence from the stratosphere. An atmospheric chemistry general circulation model is then used to simulate tropospheric ozone production above North America to gauge the impact of lightning NO_x emissions on the upper tropospheric ozone enhancement. We then examine the transport patterns that maintain the upper tropospheric ozone maximum and its interannual variability. Finally, we employ a radiative transfer model to estimate the influence of the ozone maximum on the adjusted radiative forcing at the tropopause above the southern United States.

2. Method

[7] The 410 ozone profiles utilized in this study were measured exclusively by balloon-borne ozonesondes equipped with electrochemical concentration cell sensors that have an accuracy of about 10% in the troposphere [*Newchurch et al.*, 2003; *Thompson et al.*, 2007a; *Smit et al.*, 2007]. Table 1 lists each of the 14 ozonesonde sites, the number of profiles and the launch periods. Most of the profiles (96%) occurred during August 2006, with a few occurring in late July or early September. To maximize the sample size, three of the sites contain a combination of profiles from nearby sites: Texas Coast contains profiles from downtown Houston and the research vessel *R. H. Brown* that patrolled nearby Galveston Bay and adjoining portions of the Texas coast; Ontario has profiles from the towns of Walsingham and Egbert (190 km apart); Mid-Atlantic has profiles from Beltsville, Maryland and Wallops Island, Virginia (170 km apart).

[8] The FLEXPART Lagrangian particle dispersion model was used to determine the transport histories of the air masses sampled by each ozonesonde as well as the quantity of ozone that originated in the stratosphere over the previous 20 d [*Stohl et al.*, 1998, 2005]. The model calculates the

Table 1. Summary of Upper Tropospheric FTO_3 Measurements Above North America During Summer 2006 and Summer 2004[a]

Site (With Abbreviation)	Dates in 2006	Number of Profiles in 2006	2006 10–11 km Median FTO_3 (Standard Deviation)	2006 >6 km Median FTO_3 (Standard Deviation)	2004 10–11 km FTO_3 (Standard Deviation)	2004 >6 km FTO_3 (Standard Deviation)
Barbados (BAR)	26 Jul to 30 Aug	25	50 (12)	58 (17)	NA	NA
Boulder (BOU)	26 Jul to 31 Aug	32	53 (20)	54 (18)	NA	NA
Bratt's Lake (BRA)	1–30 Aug	29	36 (33)	52 (25)	NA	NA
Huntsville (HUN)	29 Jul to 29 Aug	30	87 (17)	78 (22)	66 (24)	61 (30)
Kelowna (KEL)	2–30 Aug	27	48 (27)	50 (22)	NA	NA
Mexico City (MEX)	22 Aug to 15 Sep	21	58 (11)	57 (15)	NA	NA
Mid-Atlantic (MDA)	1–30 Aug	23	74 (17)	69 (20)	64 (31)	64 (30)
Ontario (ONT)	1–30 Aug	35	52 (24)	56 (22)	58 (24)	59 (20)
Narragansett (NAR)	27 Jul to 30 Aug	29	53 (28)	54 (23)	68 (23)	63 (25)
Sable Island (SAB)	1–31 Aug	28	71 (20)	65 (21)	56 (23)	58 (19)
Socorro (SOC)	1–25 Aug	25	63 (21)	63 (19)	NA	NA
Table Mtn (TAB)	1–31 Aug	31	35 (22)	40 (24)	48 (23)	45 (26)
Texas coast (TXC)	1–31 Aug	44	75 (20)	76 (21)	73 (12)	70 (18)
Trinidad Head (TRI)	27 Jul to 30 Aug	31	43 (23)	42 (20)	39 (23)	45 (24)

[a]Summer 2004 data from *Cooper et al.* [2006].

trajectories of a multitude of particles and was driven by ECMWF wind fields with a temporal resolution of 3 h (analyses at 0000, 0600, 1200, 1800 UTC; 3-h forecasts at 0300, 0900, 1500, 2100 UTC), horizontal resolution of $1^\circ \times 1^\circ$, and 90 vertical levels. Nested ECMWF windfields of 0.36° resolution and 90 vertical levels were used for the area between 108–27°W and 9–54°N. Particles are transported both by the resolved winds and parameterized subgrid motions. To account for convection, FLEXPART uses the parameterization scheme of *Emanuel and Živković-Rothman* [1999], which is implemented at each 15-min model time step, and is intended to describe all types of convection. Verified by *Forster et al.* [2007], the scheme produces convective precipitation amounts that are in relatively good agreement with observations both in the tropics and extratropics. It also improves the agreement of FLEXPART simulations with airborne tracer measurements compared to simulations without the convection parameterization.

[9] FLEXPART simulates well stratosphere-to-troposphere transport processes, and has been used to determine a 15-year global climatology of stratospheric intrusions [*James et al.*, 2003]; the morphology and lifetimes of midlatitude stratospheric intrusions that penetrate all the way to the lower troposphere and marine boundary layer above the tropical North Pacific Ocean [*Cooper et al.*, 2005]; and the influence of stratospheric ozone on the upper troposphere above North America [*Cooper et al.*, 2006]. In the present study the quantity of stratospheric ozone impacting each ozone profile in the troposphere was calculated using the FLEXPART retroplume technique [*Stohl et al.*, 2003], as described by *Cooper et al.* [2006]. Briefly, 40,000 back trajectory particles were released from each 500 m layer of each ozone profile. The number of particles that entered the stratosphere over the previous 20 d was tabulated along with their potential vorticity (PV) values. To estimate the amount of stratospheric ozone carried by each particle, the mass of each particle was scaled by the O_3/PV ratio of the lower stratosphere, as determined from the ozonesondes and ECMWF analyses. To account for the fact that the PV value for a given particle changes over time this calculation was averaged over each day that the particles were in the stratosphere. Once the particles left the stratosphere the ozone was allowed to decay with a 90-d e-folding lifetime. These values were integrated over all 40,000 particles in a given retroplume to yield the quantity of stratospheric ozone influencing a particular 500 m layer of an ozone profile. To verify the modeled results, the ratio of modeled/measured ozone values was calculated for all IONS ozonesonde profiles for each 500 m layer in the stratosphere (PV > 2). The geometric mean of all the point-by-point ratios of modeled/measured ozone was 0.95. A correction was applied to remove this small (5%) low bias. The standard error of the modeled stratospheric ozone compared to measured ozone was a factor of 1.5, similar to the standard error reported in other FLEXPART studies [*Cooper et al.*, 2005, 2006]. Overall the influence from the stratosphere was similar during 2006 and 2004, with slightly more influence above Ontario and Sable Island during 2006 [*Cooper et al.*, 2006].

[10] The ECHAM5/MESSy1 atmospheric chemistry general circulation model [*Jöckel et al.*, 2006] was used to calculate ozone at 250 hPa above North America during the summers of 2004 and 2006. The Modular Earth Submodel System (MESSy) describes atmospheric chemistry and meteorological processes in a modular framework for the lower and middle atmosphere up to an altitude of 80 km, and applies a relatively high resolution around the tropopause of about 500 m. The chemical mechanism includes 104 gas phase species and 245 reactions including heterogeneous reactions on sulfate aerosol and PSC-particles calculated by the MECCA submodel. The model includes biogenic emissions, anthropogenic surface emissions, aircraft emissions and 2.2 Tg a^{-1} of global lightning NO_x emissions. MESSy is coupled to the ECHAM5 general circulation model with $2.8^\circ \times 2.8^\circ$ horizontal resolution, 90 vertical levels from the surface to 0.01 hPa, and a 15-min time step [*Giorgetta et al.*, 2006]. The model is nudged toward the analysis data from the European Center for Medium-Range Weather Forecasting operational forecast model [*Lelieveld et al.*, 2007].

[11] A radiative transfer model [*Portmann and Solomon*, 2007] was used to calculate the adjusted radiative forcing at the tropopause above Huntsville, Alabama in comparison to the upwind sites. In this study adjusted radiative forcing is a measure of the extra heat (in W m^{-2}) input into the troposphere due to the changes in ozone and is found by computing the negative of the change in flux at the tropopause

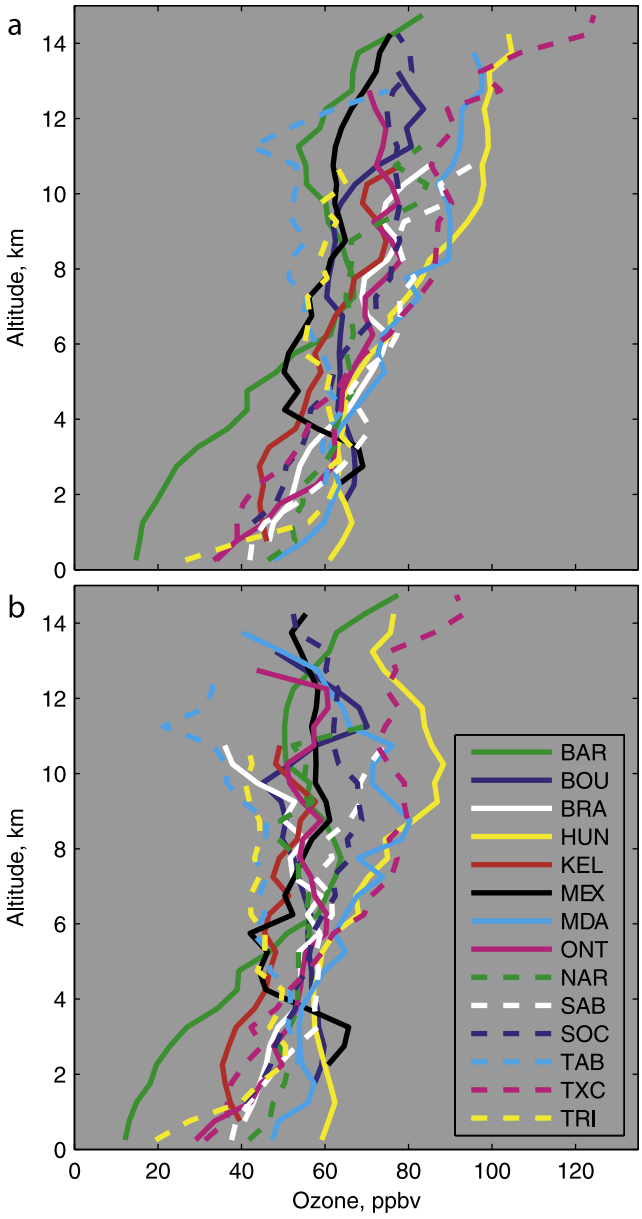

Figure 1. (a) Median ozone profiles for all measurements during summer 2006 that occurred within the troposphere (PV < 1.0 pvu). (b) Same as in Figure 1a but for the FTO3 quantity which has the influence from stratospheric-origin ozone removed.

after stratospheric temperatures have relaxed to the perturbation. The stratospheric adjustment is usually computed using the fixed dynamical heating (FDH) approximation. If stratospheric temperatures are not adjusted then the forcing is called the instantaneous radiative forcing. A line-by-line (LBL) radiative transfer model is used [*Portmann et al.*, 1997] to compute the instantaneous radiative forcing. Then the stratospheric temperatures are relaxed using the FDH approximation and a time-marching relaxation technique using the longwave heating rate changes output from the LBL calculation. The radiative forcing model used in the stratospheric adjustment calculation is the CCM-IR2 code [*Briegleb*, 1992]. The calculations used cloud parameters obtained from the ISCCP data set [*Rossow and Schiffer*, 1999], and line parameters obtained from the HITRAN 2000 compilation [*Rothman et al.*, 2003], including later corrections.

[12] Our methodology for computing the adjusted radiative forcing at the tropopause above Huntsville is as follows. First, using unfiltered ozonesonde measurements, median ozone, temperature, and humidity profiles were constructed for Huntsville, and the upwind site of Table Mountain during August 2006 between the surface and 35 km. The upper tropospheric ozone profile above Huntsville during 2006 was perturbed so that the ozone was set equal to the upper tropospheric ozone above the upwind site of Table Mountain. The unperturbed and perturbed Huntsville 2006 ozone profiles were input into the radiative transfer model to compute the adjusted radiative forcing above Huntsville due to the upper tropospheric ozone enhancement.

3. Results

3.1. Upper Tropospheric Ozone Distribution Above North America

[13] A list of the fourteen ozonesonde sites and their three-letter identifiers used throughout this study are presented in Table 1. Figure 1a shows the median ozone values at these sites, for profiles measured only within the troposphere, defined as the region of the atmosphere with isentropic potential vorticity values less than 1 potential vorticity unit (pvu). In general, the median tropospheric ozone profiles in Figure 1a show less ozone in the upper troposphere at the upwind sites of Table Mountain, Barbados, Trinidad Head and Mexico City. The greatest upper tropospheric ozone values are found in eastern North America at the Texas Coast, Huntsville, Mid-Atlantic and Sable Island sites. Upper tropospheric ozone is clearly enhanced above eastern North America, but how much of this ozone is actually produced within the troposphere?

[14] We have been conservative in our definition of the troposphere, which does not consider the 2–3 km thick transition layer that exists between the troposphere and stratosphere [*Hoor et al.*, 2002; *Pan et al.*, 2004]; this definition also filters out fresh stratospheric intrusions. However regions of the troposphere with pvu values less than 1 can still contain relatively large quantities of aged stratospheric ozone, especially in the upper troposphere. This stratospheric influence confounds our ability to quantify the ozone at each site that is produced within the troposphere. For example, on the west coast upper tropospheric (>6 km) ozone has a north–south gradient, with greater values at Kelowna, British Columbia, lower values at Trinidad Head in northern California and lower values still at Table Mountain in southern California (the location of each site is shown in Figure 2a). As would be expected, and as will be shown below, much of this gradient is due to a stronger stratospheric influence at higher latitudes.

[15] Figure 1b shows the median ozone values at each site once the stratospheric influence as calculated by FLEXPART has been removed. This quantity of ozone that has been filtered for stratospheric ozone is termed filtered tropospheric ozone (FTO_3). The ozone in these profiles was either produced in the troposphere or has an aged and well-mixed stratospheric origin greater than 20 d old. The median FTO_3 values for the upper troposphere (>6 km) are reported for each site in Table 1. At all sites the FTO_3 values

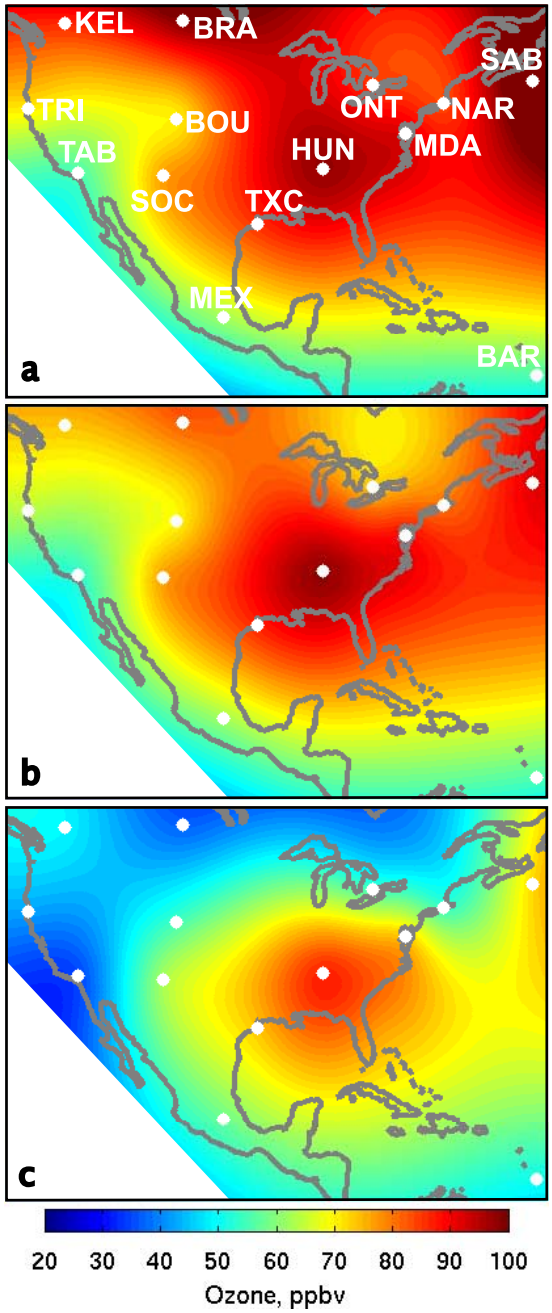

Figure 2. Median ozone mixing ratios during August 2006 at all 14 measurement sites between 10 and 11 km for (a) all measurements regardless of location in the troposphere or stratosphere, (b) measurements only within the troposphere (PV < 1 pvu), and (c) measurements only within the troposphere less the calculated quantity of ozone from the stratosphere (FTO3).

are less than the unfiltered values, with the greatest reductions at the northern sites which are closer to the polar jet stream and the associated stratospheric intrusions. The median quantity of stratospheric ozone within the troposphere above 6 km ranged from 3 ppbv at Barbados to 20 ppbv at Bratt's Lake.

[16] To illustrate the distribution of the FTO_3 above North America we focus on the 10–11 km layer which has the greatest contrast in FTO_3 mixing ratios from west to east and is the highest layer for which we have adequate data availability within the troposphere at the three west coast sites. Figure 2a is a contour plot of the median 10–11 km ozone values produced solely from the unfiltered ozone measurements at the 14 measurement sites. Figure 2a is only for broad illustrative purposes and while it depicts the large-scale ozone distribution, the interpolation of data between widely spaced data points means little emphasis should be placed on the exact location of these features, especially the smooth ozone gradient between Huntsville and Barbados. Because Figure 2a contains measurements made in both the troposphere and stratosphere, the greatest values are along the northern boundary because of both a common occurrence of low tropopause heights and frequent stratospheric intrusions. Despite its southerly location, Huntsville exhibits a distinct regional peak in ozone. Figure 2b contours the ozone measurements that were made just within the troposphere. The greatest values are above Huntsville, with an enhancement extending up the east coast. When just the FTO_3 values are contoured (Figure 2c) the east coast enhancement is much weaker, but the greatest FTO_3 values are still above Huntsville (87 ppbv). In comparison to the five upwind sites of Barbados, Mexico City, Table Mountain, Trinidad Head and Kelowna, the Huntsville FTO_3 enhancement in the 10–11 km layer ranges from 29 ppbv (compared to Mexico City) to 52 ppbv (compared to Table Mountain). When considering the entire upper troposphere (>6 km) the FTO_3 enhancement above Huntsville ranges from 20 ppbv (compared to Barbados) to 38 ppbv (compared to Table Mountain), as shown in Table 1.

3.2. Supporting Evidence From a Chemical Transport Model

[17] For the 2006 time period we conducted a simulation of North American tropospheric and stratospheric ozone using the ECHAM5/MESSy1 atmospheric chemistry general circulation model, with the standard run including 2.2 Tg a^{-1} global lightning NO_x emissions [*Jöckel et al.*, 2006]. Results from the standard run are shown in Figure 3, depicting average August 2006 ozone at 250 hPa from all sources (Figure 3a), from just the stratosphere (Figure 3b) and from all tropospheric sources (Figure 3c). Figure 3c was produced by subtracting the stratospheric component from the distribution of ozone from all sources to leave the tropospheric component. Figure 3c is not directly comparable to the FLEXPART calculated FTO_3 in Figure 2c for two reasons: (1) The FTO_3 ozone quantity can still contain very aged and well mixed stratospheric ozone older than 20 d and (2) the FTO_3 in Figure 2c is averaged just for the times when the measurements were made within the troposphere, while the ECHAM5/MESSy1 results are averaged over all times in August 2006, regardless of whether or not the 250 hPa surface was in the troposphere or stratosphere. As a result the tropospheric ozone values at high latitudes in Figure 3c are very low because the 250 hPa surface in this region is often in the stratosphere.

[18] While Figure 2c and Figure 3c are not directly comparable, the ECHAM5/MESSy1 results in Figure 3c confirm the presence of an upper tropospheric ozone maximum above the southern USA. However, the

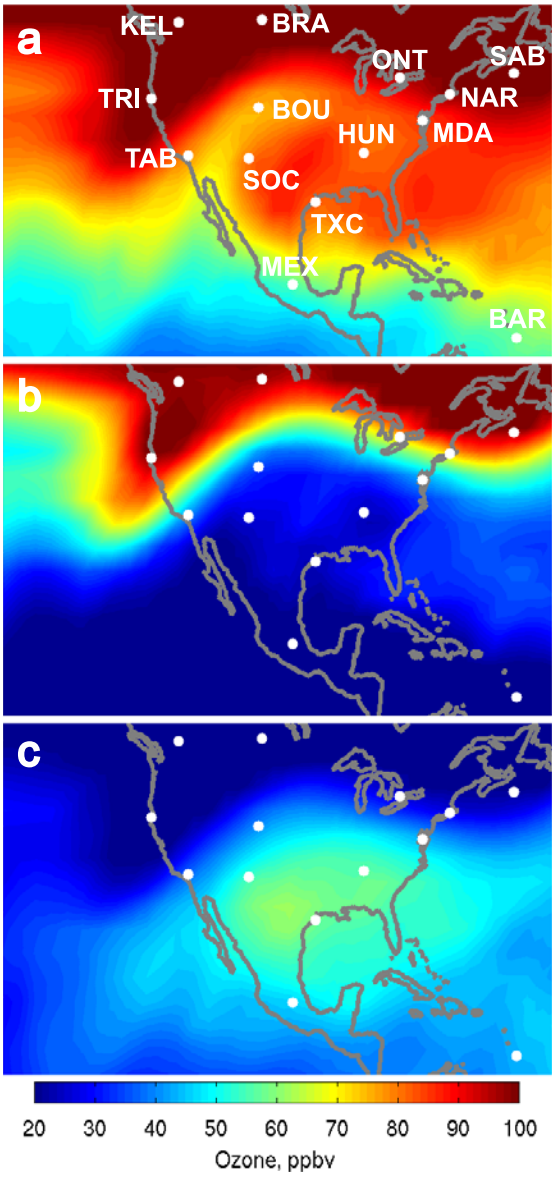

Figure 3. Model calculated (a) mean ozone mixing ratios at 250 hPa during August 2006, subdivided into (b) the contribution of ozone transported from the stratosphere and (c) the contribution of ozone formed within the troposphere (thus Figure 3a = Figure 3b + Figure 3c). Note stratospheric conditions prevail north of the jet stream (north of strong ozone gradients) and tropospheric conditions to the south.

ECHAM5/MESSy1 model places the ozone maximum above Texas rather than Huntsville, and the maximum upper tropospheric ozone values are 60–65 ppbv, much less than the 87 ppbv FTO_3 above Huntsville. Part of the discrepancy could be due to the very aged stratospheric ozone still present in the FTO_3 quantity. However, most of the discrepancy can be explained by an underestimate of lightning NO_x in the standard model simulation, as confirmed by the analysis of *Tost et al.* [2007], which indicates that the standard model underestimates the lightning flash frequency associated with the American monsoon convection.

[19] We conducted 2 sensitivity tests to gauge the impact of lightning NO_x on the upper tropospheric ozone enhancement. The first sensitivity test set global lightning NO_x emissions to zero. The result is still an ozone maximum above the southern USA, in agreement with the calculations made by *Cooper et al.* [2006], but ozone mixing ratios are quite low at 40–50 ppbv (Figure 4a). The source for the more modest ozone enhancement is direct transport of ozone from the surface to the upper troposphere and in situ production of ozone from anthropogenic and biogenic NO_x emissions that recirculate in the upper tropospheric anticyclone. The second sensitivity test increased global lightning NO_x emissions from 2.2 Tg a^{-1} to 6.6 Tg a^{-1}. The extra NO_x enhanced the ozone maximum above the southern USA compared to the standard run and produced maximum ozone values in the 65–75 ppbv range. These values are close to the 75 ppbv FTO_3 above the Texas Coast, but still less than the 87 ppbv FTO_3 at 10–11 km above Huntsville. While lightning NO_x emissions of 6.6 Tg a^{-1} are within the currently accepted range of 5 ± 3 Tg a^{-1} [*Schumann and Huntrieser*, 2007], the North American modeled lightning NO_x emissions may still be underestimated, as discussed by *Hudman et al.* [2007]. Comparison between the two sensitivity tests indicates that lightning NO_x contributes 25–30 ppbv of ozone to the upper tropospheric ozone maximum above the southern USA.

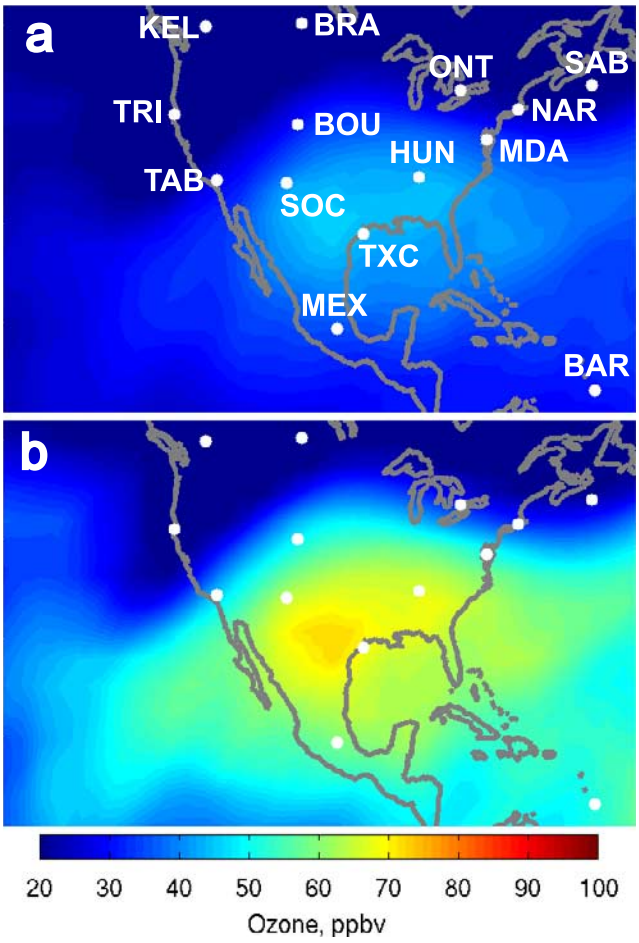

Figure 4. As in Figure 3c but for (a) global lightning emissions set to zero and (b) global lightning emissions increased by a factor of 3.

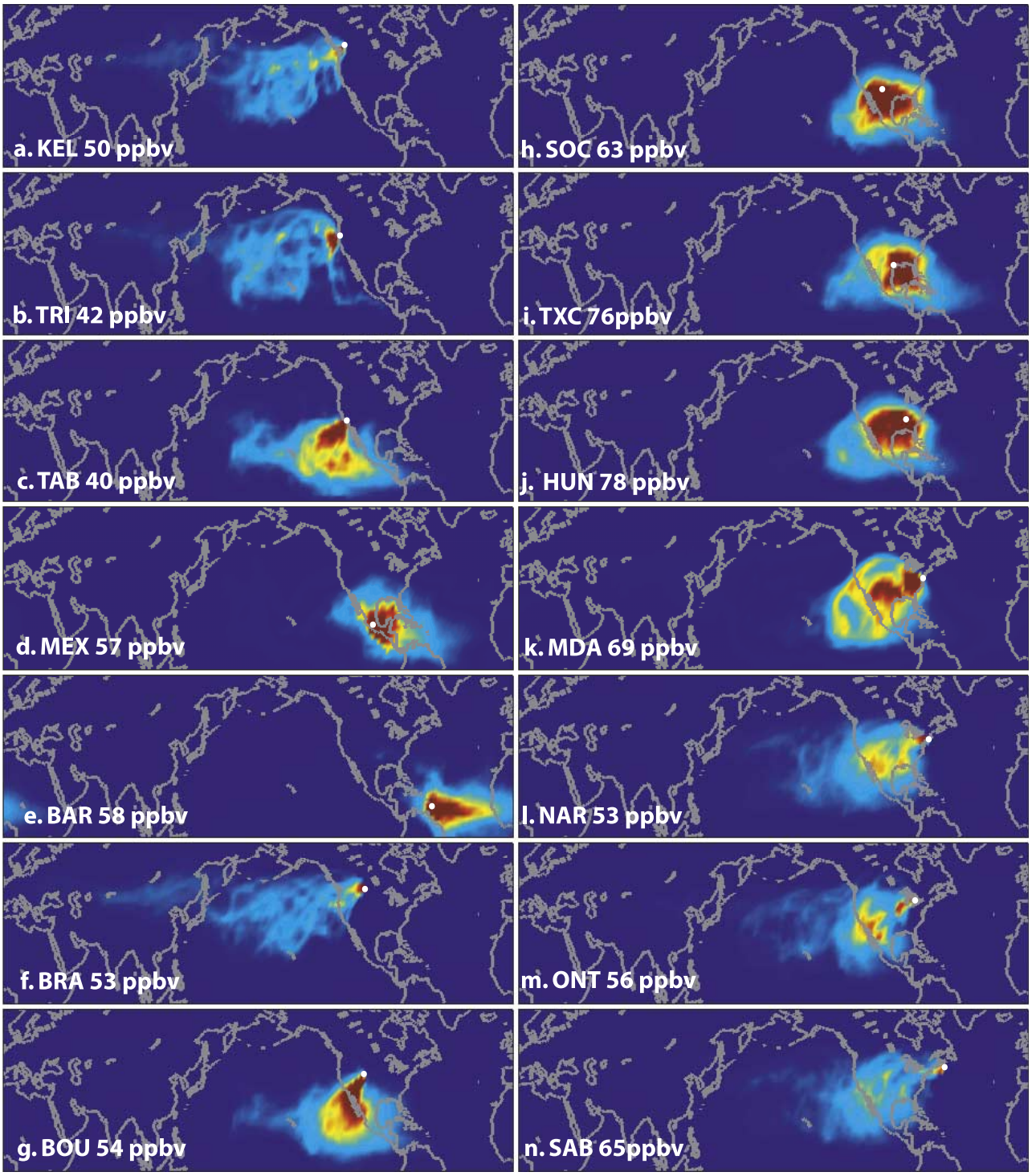

Figure 5. Average column residence time (arbitrary units) for all retroplumes released between 6 and 12 km within the troposphere above each site (white dot): (a) Kelowna, (b) Trinidad Head, (c) Table Mountain, (d) Mexico City, (e) Barbados, (f) Bratt's Lake, (g) Boulder, (h) Socorro, (i) Texas coast, (j) Huntsville, (k) Mid-Atlantic, (l) Narragansett, (m) Ontario, and (n) Sable Island. Each plot also indicates the median FTO3 mixing ratio between 6 and 12 km above each site.

3.3. Influence of Transport Patterns on the Ozone Maximum

[20] The North American Monsoon and the upper tropospheric anticyclone dominate transport patterns above southern and eastern North America during summer and play a key role in producing the upper tropospheric ozone maximum. We illustrate the influence of transport with Figure 5, which shows the mean column pathways of all FLEXPART retroplumes released within the upper troposphere (6–12 km) above the 14 measurement sites, orga-

nized to first show the upwind sites from north to south (Figures 5a–5e), followed by the inland western North America sites (Figures 5f–5h), the southern USA sites (Figures 5i–5j) and finally the sites in the northeast USA and eastern Canada (Figures 5k–5n). Beginning at the west coast we find the lowest upper tropospheric FTO_3 values of all 14 sites are above Table Mountain (40 ppbv). Figure 5c shows that the main source region is the subtropical and tropical eastern Pacific. In contrast the most northerly west coast site, Kelowna (50 ppbv), has an average retroplume that crosses midlatitude Asia and the North Pacific Ocean (Figure 5a), resulting in an extra 10 ppbv FTO_3. Trinidad Head which lies between Kelowna and Table Mountain has FTO_3 (42 ppbv) similar to Table Mountain but a transport pathway (Figure 5b) more similar to Kelowna. However, Trinidad Head does have a greater frequency of transport events from the lower tropical troposphere than Kelowna, resulting in a greater number of low FTO_3 events above Trinidad Head, while Kelowna has a greater influence from the lower troposphere of Europe and Asia resulting in more pollution episodes above Kelowna. Overall these three west coast sites have the lowest upper tropospheric FTO_3 mixing ratios of all 14 sites, as expected given their location upwind of fresh North American emissions.

[21] Continuing with our analysis of sites upwind of eastern North America we find the upper troposphere above Barbados has more FTO_3 (58 ppbv) than the west coast sites. This is a very important upwind site, carefully chosen to characterize the background ozone entering North America from the tropical North Atlantic Ocean and Africa (Figure 5e). The final upwind site, Mexico City, is located west of Barbados with similar FTO_3 mixing ratios (57 ppbv), but a source region primarily influenced by Central America and the Gulf of Mexico (Figure 5d). It is interesting to note that these two southerly sites have greater ozone mixing ratios than the west coast sites that have a stronger influence from Asian emissions. Mexico City is influenced by ozone production from the widespread lightning above Central America (Figure 4), while Barbados appears to receive influence from ozone produced from lightning emissions in tropical Africa that are comparable in magnitude to North America during June, July and August [*Christian et al.*, 2003].

[22] Focusing now on the three inland sites of western North America, Bratt's Lake in southern Canada has FTO_3 (52 ppbv) and transport pathways (Figure 5f) similar to Kelowna. On the eastern edge of the Rocky Mountains FTO_3 above Boulder is 54 ppbv, 12–14 ppbv greater than Trinidad Head and Table Mountain to the west. The Boulder air masses either originate over the subtropical and tropical eastern Pacific, or are influenced by the North American Monsoon which advects lightning NO_x emissions northward into the southern USA along the Rocky Mountains on the western edge of the semipermanent upper tropospheric anticyclone (Figure 5g). The increase in FTO_3 compared to the west coast sites is mainly due to the influence from the monsoonal flow. In contrast, the Socorro, New Mexico site south of Boulder is almost entirely affected by the monsoon flow. Socorro has 9 ppbv more FTO_3 (median value of 63 ppbv) than Boulder, and 23 ppbv more FTO_3 than Table Mountain located directly to the west. The increase of FTO_3 (6 ppbv) between Mexico City and Socorro is mainly attributed to ozone production within the upper troposphere as air masses move northward with the monsoon flow and recirculate above southern North America (Figure 5h), as indicated by the ECHAM5/MESSy1 model (Figure 4b). This result shows that the western boundary of the upper tropospheric ozone maximum is embedded within the North American monsoon flow.

[23] The two sites with the highest FTO_3 are Texas Coast (76 ppbv) and Huntsville (78 ppbv) and as described above are heavily influenced by ozone production within the upper tropospheric anticyclone, which mainly keeps the upper tropospheric air masses circulating above the southern USA and the Gulf of Mexico (Figures 5i and 5j). Moving northeastward away from Huntsville the influence from the anticyclone decreases and FTO_3 values are lower above the Mid-Atlantic site (69 ppbv), Ontario (56 ppbv), Narragansett (54 ppbv) and Sable Island (65 ppbv). All four sites have broadly similar transport pathways, however one major difference is that when the retroplumes come in contact with the surface, western North America has the strongest influence on Ontario (56 ppbv) and Narragansett (54 ppbv), while the heavily populated and more polluted eastern USA has more influence on the Mid-Atlantic site (69 ppbv) and Sable Island (65 ppbv).

3.4. Interannual Variability of the Upper Tropospheric Ozone Maximum

[24] Southeastern North America is one of Earth's two main lightning regions during boreal summer, the other being tropical Africa [*Christian et al.*, 2003]. Much of the North American lightning occurs within the annually recurring upper tropospheric anticyclone. Therefore, on the basis of the studies of *Li et al.* [2005] and *Cooper et al.* [2006] we hypothesized that the upper tropospheric ozone maximum should be a recurring feature during summertime above North America, and that a stronger upper level anticyclone should result in a greater upper tropospheric ozone maximum because the recirculating air masses within the anticyclone would have more time to accumulate ozone precursors, and more days to experience photochemical ozone production.

[25] While the summer 2004 IONS ozonesonde study had a more limited distribution of measurement sites, especially above western North America, we compare the ozone mixing ratios between the two studies where possible (Table 1). The 2004 summertime upper tropospheric (>6 km) FTO_3 maximum was located above Houston (70 ppbv). In 2006 the maximum was located above Huntsville with a median upper FTO_3 value of 78 ppbv, which is 17 ppbv greater than Huntsville's 2004 value and 8 ppbv greater than the 2004 Houston value. Both the shift of the ozone maximum from Houston in 2004 to Huntsville in 2006, and the greater FTO_3 values in 2006, are due to the strength and location of the upper tropospheric anticyclone. Figure 6 shows the average 250 hPa geopotential height and wind barbs for the 2004 and 2006 summertime study periods. In 2004 the upper tropospheric anticyclone was established above northern Mexico and the northern Gulf of Mexico, with Houston being the measurement site closest to the center of the anticyclone. In 2006 the center of the anticyclone had shifted to the northeast so that it was closer to Huntsville.

[26] The stronger anticyclonic circulation of 2006 also increased the time that air masses spent recirculating above

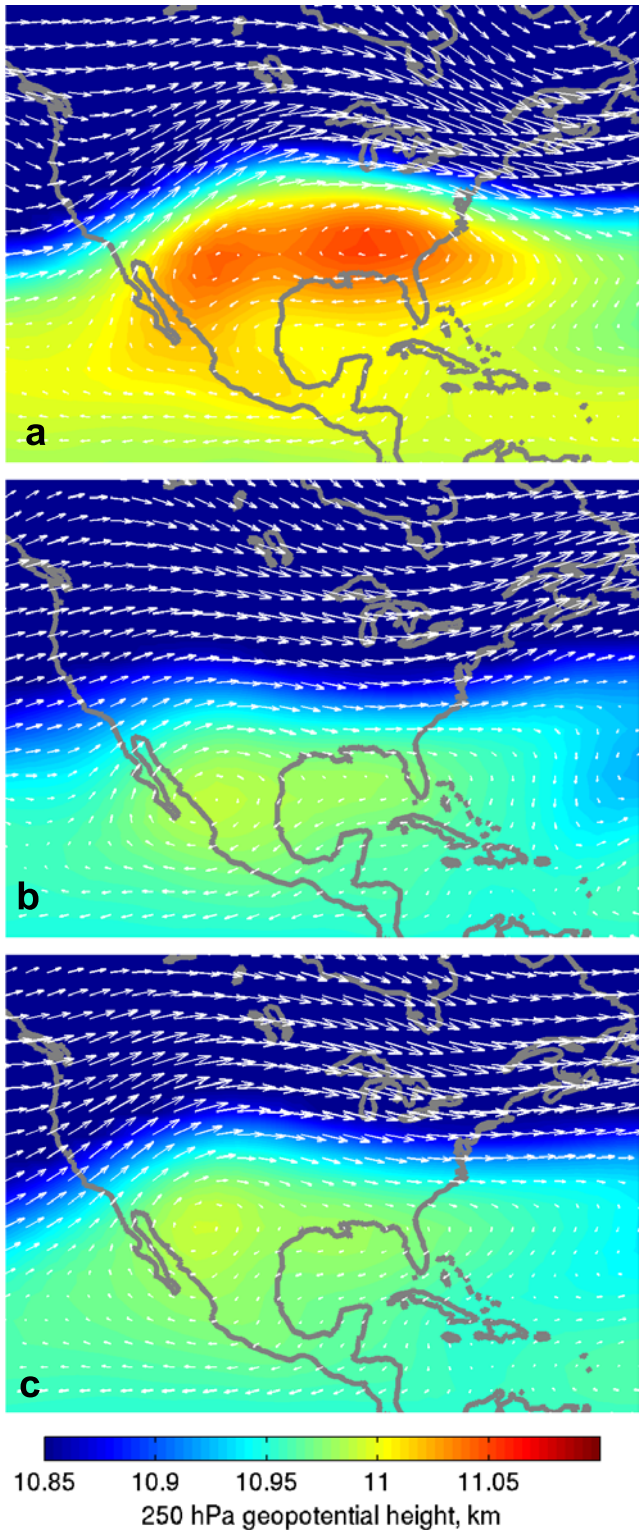

Figure 6. Average wind vectors and geopotential height of the 250 hPa surface above North America during (a) August 2006, (b) July–August 2004, and (c) July–August 1987–2006.

the southeastern USA. Figure 7 shows the relative upper tropospheric residence time of the FLEXPART retroplumes released from the upper troposphere above Huntsville in 2004 and 2006. In 2004 the upper troposphere above Huntsville had a strong influence from the southeastern USA but also had a broad impact from air masses that originated above the North Pacific Ocean. In contrast the air masses in 2006 spent much more time above the southeastern USA and had less influence from the Pacific. The average residence time of these air parcels above the southeastern USA increased by 79% from 2004 to 2006, corresponding to an increase in FTO_3 of 17 ppbv. Above the Texas Coast, the residence time of air parcels in the upper troposphere of the southeastern USA increased by 17% from 2004 to 2006, corresponding to an FTO_3 increase of 6 ppbv. During 2006 the residence time of Huntsville air parcels above the southeastern USA was 14% greater than for Texas Coast air parcels, corresponding to an extra 2 ppbv of FTO_3 at Huntsville. In contrast, Huntsville air parcels in 2004 spent 24% less time above the southeastern USA than Houston air parcels, corresponding to 9 ppbv less FTO_3 above Huntsville.

[27] Because the air masses associated with the ozone enhancement above Huntsville spent longer time periods within the upper level anticyclone than air masses associated with any other site in 2006 or 2004 there was even more time for in situ photochemical ozone production. The result was the greatest FTO_3 mixing ratios (median value of 78 ppbv) of any site in 2004 or 2006. Simulations of upper tropospheric ozone using the ECHAM5/MESSy1 model also indicate that the broad features of the upper tropo-

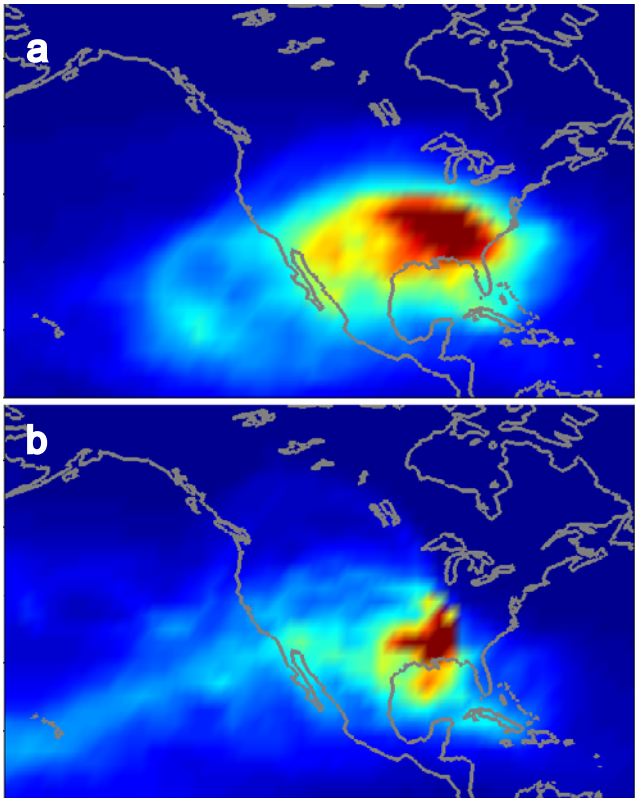

Figure 7. Average residence time (in arbitrary units) in the upper troposphere of all retroplumes released between 6 and 12 km above Huntsville during (a) August 2006 and (b) July–August 2004.

spheric ozone enhancement shift with the anticyclonic circulation at 250 hPa from year to year.

[28] Figure 6c shows the average location of the 250 hPa geopotential height surface for July and August over the 1987–2006 time period. The location of the climatological anticyclone is intermediate between the positions in 2006 and 2004. Therefore the maximum ozone values being located above Huntsville in 2006 are probably not typical. In a more typical year the ozone maximum is more likely to be located closer to the northern coast of the Gulf of Mexico. Also the climatological anticyclonic circulation is not as strong as in 2006 so the upper tropospheric FTO_3 maximum of 78 ppbv above Huntsville in 2006 is probably greater than average. It is likely that more typical mixing ratios would be similar to those found above Houston in 2004 (70 ppbv).

4. Discussion: Implications for the Radiation Budget

[29] Because of ozone's role as an important greenhouse gas, we briefly explore implications the FTO_3 maximum could have for the radiation budget of the southeastern United States. Compared to the upwind site of Table Mountain, Huntsville has an extra 11 Dobson Units (DU) of ozone in the upper troposphere. This enhancement is 20% of the tropospheric column of ozone above Huntsville and occurs in the region where ozone has the strongest influence on radiative forcing [*Forster and Shine*, 1997]. We ran a radiative transfer model and calculated that the ozone enhancement above Huntsville produces a positive all-sky adjusted radiative forcing at the tropopause of 0.50 W m^{-2} in comparison to Table Mountain. Comparison to Table Mountain, the site with the lowest values of FTO_3 means that 0.50 W m^{-2} is the largest expected radiative forcing. This positive radiative forcing is less than half a percent of the outgoing longwave radiation of 242 W m^{-2}, and less than the reduction in solar irradiance caused by aerosols which can peak at 60–70 W m^{-2} above the southeastern USA during summertime stagnation events [*Zamora et al.*, 2003]. Such a radiative forcing would be important for the global radiation budget if it were of anthropogenic origin and applied to the global scale (compare to the 0.35 W m^{-2} global average radiative forcing of ozone from anthropogenic influences [*Intergovernmental Panel on Climate Change*, 2007]). However, the implications of this regional-scale ozone enhancement with a large natural component are less clear.

5. Conclusions

[30] The IONS summer 2006 experiment provided 410 ozone profiles across North America, yielding the best in situ view of the continent's free tropospheric ozone distribution ever achieved during a single season. The study confirmed the hypothesis that the upper tropospheric FTO_3 maximum above eastern North America is a recurring summertime feature and that its exact location and strength varies interannually with the mean location and strength of the upper tropospheric anticyclone. The enhancement of FTO_3 above Huntsville was 20–38 ppbv in comparison to five upwind sites for the entire upper troposphere (>6 km), and 29–52 ppbv for just the 10–11 km layer. Our modeling work indicates that lightning NO_x led to the production of 25–30 ppbv ozone at 250 hPa (approximately the 10–11 km layer) above the southern United States during August 2006. However, the anomalously strong anticyclonic circulation during summer 2006 suggests that the overall FTO_3 enhancement is greater than in more typical years. The data also show that the western boundary of the FTO_3 enhancement is maintained by the southerly flow of the North American Monsoon. On the regional scale the ozone enhancement above the southeastern United States can produce a positive all-sky adjusted radiative forcing up to 0.50 W m^{-2}. The ozonesonde network presented in this study demonstrates the great value of high temporal and spatial resolution measurements and can serve as a model for the design of a future hemispheric or global-scale ozone monitoring network.

[31] While this study and others have made good progress in identifying the presence of the upper tropospheric ozone enhancement above the summertime USA and establishing a strong relationship to lightning NO_x emissions, many questions still remain. We conclude this paper by posing five science questions for future research:

[32] 1. What are the detailed chemical mechanisms that produce the FTO_3 maximum and its buildup and decay over the course of a year? In situ measurements that could help answer this question will be gathered in summer 2010 when a consortium of universities and government agencies plans to use two jet aircraft to survey the impact of convection and lightning on the chemistry of the upper troposphere of the southern United States (Deep Convective Clouds and Chemistry Experiment (DC3)).

[33] 2. Does the regional-scale radiative forcing of the ozone enhancement impact surface temperatures which could produce feedbacks between convection, lightning and ozone production in the upper troposphere? This question could be addressed with coupled chemistry-climate models.

[34] 3. What is the impact of this ozone enhancement on the summertime northern hemisphere ozone budget and is the feature reproduced by chemical transport models and global climate models?

[35] 4. Recent studies suggest anthropogenic activity through urban heat island effects and/or aerosol production can increase lightning frequency near urban areas in the southern USA [*Orville et al.*, 2001; *Steiger and Orville*, 2003; *Smith et al.*, 2005; *Stallins et al.*, 2006]. What is the impact of anthropogenic activity through modification of lightning frequency as well as through past climate change on the intensity and location of the upper tropospheric ozone enhancement above the southern United States?

[36] 5. Finally, anthropogenic emissions are expected to warm the atmosphere during the 21st century, which may increase convective activity and lightning NO_x emissions [*Hauglustaine et al.*, 2005]. How will future climate change impact this upper tropospheric ozone feature?

[37] **Acknowledgments.** Funding of the August 2006 IONS ozonesondes was provided by Environment Canada; NOAA; NASA; U.S. EPA; Max Plank Institute for Chemistry, Mainz; Los Alamos National Laboratory; Valparaiso University; California Department of Energy; and the California Air Resources Board.

References

Briegleb, B. (1992), Longwave band model for thermal radiation in climate studies, *J. Geophys. Res.*, *97*, 11,475–11,485.

Christian, H. J., et al. (2003), Global frequency and distribution of lightning as observed from space by the Optical Transient Detector, *J. Geophys. Res.*, *108*(D1), 4005, doi:10.1029/2002JD002347.

Cooper, O. R., et al. (2005), Direct transport of midlatitude stratospheric ozone into the lower troposphere and marine boundary layer of the tropical Pacific Ocean, *J. Geophys. Res.*, *110*, D23310, doi:10.1029/2005JD005783.

Cooper, O. R., et al. (2006), Large upper tropospheric ozone enhancements above midlatitude North America during summer: In situ evidence from the IONS and MOZAIC ozone measurement network, *J. Geophys. Res.*, *111*, D24S05, doi:10.1029/2006JD007306.

Emanuel, K. A., and M. Živković-Rothman (1999), Development and evaluation of a convection scheme for use in climate models, *J. Atmos. Sci.*, *56*, 1766–1782.

Forster, C., A. Stohl, and P. Seibert (2007), Parameterization of convective transport in a Lagrangian particle dispersion model and its evaluation, *J. Appl. Meteorol. Climatol.*, *46*(4), 403–422.

Forster, P. M. de F., and K. P. Shine (1997), Radiative forcing and temperature trends from stratospheric ozone changes, *J. Geophys. Res.*, *102*, 10,841–10,857.

Giorgetta, M. A., E. Manzini, E. Roeckner, M. Esch, and L. Bengtsson (2006), Climatology and forcing of the quasi-biennial oscillation in the MAECHAM5 model, *J. Clim.*, *19*, 3882–3901.

Hauglustaine, D. A., G. P. Brasseur, S. Walters, P. J. Rasch, J.-F. Müller, L. K. Emmons, and M. A. Carroll (1998), MOZART, a global chemical transport model for ozone and related chemical tracers: 2. Model results and evaluation, *J. Geophys. Res.*, *103*, 28,291–28,335.

Hauglustaine, D. A., J. Lathière, S. Szopa, and G. A. Folberth (2005), Future tropospheric ozone simulated with a climate-chemistry-biosphere model, *Geophys. Res. Lett.*, *32*, L24807, doi:10.1029/2005GL024031.

Hoor, P., H. Fischer, L. Lange, J. Lelieveld, and D. Brunner (2002), Seasonal variations of a mixing layer in the lowermost stratosphere as identified by the CO-O_3 correlation from in situ measurements, *J. Geophys. Res.*, *107*(D5), 4044, doi:10.1029/2000JD000289.

Hudman, R. C., et al. (2007), Surface and lightning sources of nitrogen oxides over the United States: Magnitudes, chemical evolution, and outflow, *J. Geophys. Res.*, *112*, D12S05, doi:10.1029/2006JD007912.

Intergovernmental Panel on Climate Change (2001), *Climate Change 2001: The Scientific Basis—Contribution of Working Group I to the Third Assessment Report of the Intergovernmental Panel on Climate Change*, edited by J. T. Houghton et al., 881 pp., Cambridge Univ. Press, New York.

Intergovernmental Panel on Climate Change (2007), *Climate Change 2007: The Physical Science Basis, Summary for Policymakers—Contribution of Working Group I to the Fourth Assessment Report of the Intergovernmental Panel on Climate Change*, Cambridge Univ. Press, New York.

James, P., A. Stohl, C. Forster, S. Eckhardt, P. Seibert, and A. Frank (2003), A 15-year climatology of stratosphere-troposphere exchange with a Lagrangian particle dispersion model: 2. Mean climate and seasonal variability, *J. Geophys. Res.*, *108*(D12), 8522, doi:10.1029/2002JD002639.

Jöckel, P., et al. (2006), The atmospheric chemistry general circulation model ECHAM5/MESSy1: Consistent simulation of ozone from the surface to the mesosphere, *Atmos. Chem. Phys.*, *6*, 5067–5104.

Lamarque, J.-F., P. Hess, L. Emmons, L. Buja, W. Washington, and C. Granier (2005), Tropospheric ozone evolution between 1890 and 1990, *J. Geophys. Res.*, *110*, D08304, doi:10.1029/2004JD005537.

Lelieveld, J., et al. (2007), Stratospheric dryness: Model simulations and satellite observations, *Atmos. Chem. Phys.*, *7*, 1313–1332.

Levy, H., II, P. S. Kasibhatla, W. J. Moxim, A. A. Klonecki, A. I. Hirsch, S. J. Oltmans, and W. L. Chameides (1997), The global impact of human activity on tropospheric ozone, *Geophys. Res. Lett.*, *24*, 791–794.

Li, Q., D. J. Jacob, R. Park, Y. Wang, C. L. Heald, R. Hudman, R. M. Yantosca, R. V. Martin, and M. Evans (2005), North American pollution outflow and the trapping of convectively lifted pollution by upper-level anticyclone, *J. Geophys. Res.*, *110*, D10301, doi:10.1029/2004JD005039.

Marenco, A., H. Gouget, P. Nédélec, J. P. Pagés, and F. Karcher (1994), Evidence of a long-term increase in tropospheric ozone from Pic du Midi data series, *J. Geophys. Res.*, *99*, 16,617–16,632.

Newchurch, M. J., M. A. Ayoub, S. Oltmans, B. Johnson, and F. J. Schmidlin (2003), Vertical distribution of ozone at four sites in the United States, *J. Geophys. Res.*, *108*(D1), 4031, doi:10.1029/2002JD002059.

Oltmans, S. J., et al. (2006), Long-term changes in tropospheric ozone, *Atmos. Environ.*, *40*, 3156–3173.

Orville, R. E., G. Huffines, J. Nielsen-Gammon, R. Y. Zhang, B. Ely, S. Steiger, S. Phillips, S. Allen, and W. Read (2001), Enhancement of cloud-to-ground lightning over Houston, Texas, *Geophys. Res. Lett.*, *28*, 2597–2600.

Pan, L. L., W. J. Randel, B. L. Gary, M. J. Mahoney, and E. J. Hintsa (2004), Definitions and sharpness of the extratropical tropopause: A trace gas perspective, *J. Geophys. Res.*, *109*, D23103, doi:10.1029/2004JD004982.

Portmann, R. W., and S. Solomon (2007), Indirect radiative forcing of the ozone layer during the 21st century, *Geophys. Res. Lett.*, *34*, L02813, doi:10.1029/2006GL028252.

Portmann, R. W., S. Solomon, J. Fishman, J. R. Olson, J. T. Kiehl, and B. Briegleb (1997), Radiative forcing of the Earth's climate system due to tropical tropospheric ozone production, *J. Geophys. Res.*, *102*, 9409–9417.

Rossow, W. B., and R. A. Schiffer (1999), Advances in understanding clouds from ISCCP, *Bull. Am. Meteorol. Soc.*, *80*, 2261–2288.

Rothman, L. S., et al. (2003), The HITRAN Molecular Spectroscopic Database: Edition of 2000 including updates of 2001, *J. Quant Spectrosc. Radiat. Transfer*, *82*, 5–44.

Schumann, U., and H. Huntrieser (2007), The global lightning-induced nitrogen oxides source, *Atmos. Chem. Phys.*, *7*, 3823–3907.

Smit, H. G. J., et al. (2007), Assessment of the performance of ECC-ozonesondes under quasi-flight conditions in the environmental simulation chamber: Insights from the Juelich Ozone Sonde Intercomparison Experiment (JOSIE), *J. Geophys. Res.*, *112*, D19306, doi:10.1029/2006JD007308.

Smith, J. R., H. E. Fuelberg, and A. I. Watson (2005), Warm season lightning distributions over the northern Gulf of Mexico coast and their relation to synoptic-scale and mesoscale environments, *Weather Forecasting*, *20*, 415–438.

Staehelin, J., J. Thudium, R. Buehler, A. Volz-Thomas, and W. Graber (1994), Trends in surface ozone concentrations at Arosa (Switzerland), *Atmos. Environ.*, *28*, 75–87.

Stallins, J. A., M. L. Bentley, and L. S. Rose (2006), Cloud-to-ground flash patterns for Atlanta, Georgia (USA) from 1992 to 2003, *Clim. Res.*, *30*, 99–112.

Steiger, S. M., and R. E. Orville (2003), Cloud-to-ground lightning enhancement over Southern Louisiana, *Geophys. Res. Lett.*, *30*(19), 1975, doi:10.1029/2003GL017923.

Stohl, A., M. Hittenberger, and G. Wotawa (1998), Validation of the Lagrangian particle dispersion model FLEXPART against large scale tracer experiment data, *Atmos. Environ.*, *32*, 4245–4264.

Stohl, A., C. Forster, S. Eckhardt, N. Spichtinger, H. Huntrieser, J. Heland, H. Schlager, H. Aufmhoff, F. Arnold, and O. Cooper (2003), A backward modeling study of intercontinental pollution transport using aircraft measurements, *J. Geophys. Res.*, *108*(D12), 4370, doi:10.1029/2002JD002862.

Stohl, A., C. Forster, A. Frank, P. Seibert, and G. Wotowa (2005), Technical note: The Lagrangian particle dispersion model FLEXPART version 6.2, *Atmos. Chem. Phys.*, *5*, 2461–2474.

Thompson, A. M., J. C. Witte, H. G. Smit, S. J. Oltmans, B. J. Johnson, V. W. J. H. Kirchhoff, and F. J. Schmidlin (2007a), Southern Hemisphere Additional Ozonesondes (SHADOZ) 1998–2004 tropical ozone climatology: 3. Instrumentation, station-to-station variability, and evaluation with simulated flight profiles, *J. Geophys. Res.*, *112*, D03304, doi:10.1029/2005JD007042.

Thompson, A. M., et al. (2007b), Intercontinental Chemical Transport Experiment Ozonesonde Network Study (IONS) 2004: 1. Summertime upper troposphere/lower stratosphere ozone over northeastern North America, *J. Geophys. Res.*, *112*, D12S12, doi:10.1029/2006JD007441.

Tost, H., P. Jöckel, and J. Lelieveld (2007), Lightning and convection parameterizations—Uncertainties in global modeling, *Atmos. Chem. Phys. Disc.*, *7*, 6767–6801.

Zamora, R. J., S. Solomon, E. G. Dutton, J. W. Bao, M. Trainer, R. W. Portmann, A. B. White, D. W. Nelson, and R. T. McNider (2003), Comparing MM5 radiative fluxes with observations gathered during the 1995 and 1999 Nashville southern oxidants studies, *J. Geophys. Res.*, *108*(D2), 4050, doi:10.1029/2002JD002122.

T. Carey-Smith, National Institute of Water and Atmospheric Research Ltd., Private Bag 14901, Kilbirnie, Wellington, New Zealand.

O. R. Cooper, F. C. Fehsenfeld, B. J. Johnson, J. Meagher, S. J. Oltmans, R. W. Portmann, M. Trainer, and D. Wolfe, Earth System Research Laboratory, NOAA, Boulder, CO 80305, USA. (owen.r.cooper@noaa.gov)

M. K. Dubey, Los Alamos National Laboratory, Los Alamos, NM 87545, USA.

S. Eckhardt and A. Stohl, Norwegian Institute for Air Research, N-2027 Kjeller, Norway.

G. Forbes, Meteorological Service of Canada–Sable Island, 45 Alderney Drive, Dartmouth, NS, Canada B2Y 2N6.

E. Joseph, Department of Physics and Astronomy, Howard University, Washington, DC 20059, USA.

L. Kalnajs, Laboratory of Atmospheric and Space Physics, University of Colorado, Boulder, CO 80309, USA.

T. J. Keating, Office of Air and Radiation, United States Environmental Protection Agency, 1200 Pennsylvania Avenue NW, Mail Code 6103A (Room 5442), Washington, DC 20460, USA.

T. Leblanc and I. S. McDermid, Table Mountain Facility, Jet Propulsion Laboratory, California Institute of Technology, Wrightwood, CA 92397, USA.

B. Lefer and B. Rappenglück, Geosciences Department, University of Houston, Houston, TX 77204, USA.

J. Lelieveld, Max Plank Institute for Chemistry, D-55128 Mainz, Germany.

K. Minschwaner, Department of Physics, New Mexico Institute of Mining and Technology, Socorro, NM 87801, USA.

G. A. Morris, Department of Physics and Astronomy, Valparaiso University, Valparaiso, IN 46383, USA.

M. J. Newchurch, Atmospheric Science Department, University of Alabama in Huntsville, Huntsville, AL 35806, USA.

F. Schmidlin, Wallops Flight Facility, NASA Goddard Space Flight Center, Wallops Island, VA 23337, USA.

D. W. Tarasick, Experimental Studies Research Division, Meteorological Service of Canada, Environment Canada, Downsview, ON, Canada M3H 5T4.

A. M. Thompson, Department of Meteorology, Pennsylvania State University, University Park, PA 16802, USA.

R. A. Van Curen, Atmospheric Processes Research Section, Research Division, California Air Resources Board, 1001 I Street, Sacramento, CA 95812, USA.

J. C. Witte, Science Systems and Applications, Inc., NASA Goddard Space Flight Center, Greenbelt, MD 20771, USA.